Brushless self-excited single-phase synchronous generator Part I - Impact of rotor excitation modes on harmonic contents

M. Y. Abdelfattah
Electrical Engineering Dept., Faculty of Eng., Alexandria University, Alexandria , Egypt

Brushless self-excited single-phase synchronous generator (BSESPSG) is a three-phase induction machine where the stator constitute the excitation winding and load winding, while the rotor windings are connected through diodes to rectify double frequency induced voltage. The generator operates synchronously to produce output voltage where residual magnetism is needed for self-excitation. This paper presents theoretical and experimental investigation for transient and steady-state performance based on voltage equations in real machine variables. The analysis is performed for different rotor excitation modes. A good agreement between theoretical and measured results was observed.

يعتمد هذا البحث على تمثيل آلة حثية ثلاثية الأوجه بمجموعة من الملفات ترتبط معا مغناطيسيا لتوليد الجهد حيث تم توصيل العضو الدوار من خلال مقومات بطريقتين وذلك لتقويم الجهد ذات التردد المضاعف لتوليد تيار الإثارة . ويقدم البحث تحليلا نظريا للآلة يستخدم في دراسة خواص الآلة في الحالة العابرة وحالة الاستقرار عند اللاحمل أو الحمل. تم إجراء التجارب المعملية للحصول على نتائج ومقارنتها بالنتائج النظرية حيث تبين تطابق النتائج العملية مع النتائج النظرية.

Keywords: Induction machine, Brushless self-excited, Synchronous generator

1. Introduction

A large number of attempts have been made by some authors in the development of the brushless self-excited single-phase synchronous generator BSESPSG [1-5]. This is due to its various advantages over conventional synchronous generator such as simplicity in structure, no separate dc source for excitation and above all least maintenance. Ref. [1] presented the original BSESPSG and studied the analysis at no load only while neglecting machine resistance and action of diodes in the rotor circuit. On the other hand, ref. [2] proposed a three phase induction motor of slip ring type to replace reference [1] system as shown in fig. 1. Two stator phases are connected at their neutral point to act as the load winding. The remaining phase serves as the excitation winding where a capacitor is used to supply the necessary leading reactive power.

Ref. [3] presented a self-excited single-phase synchronous generator. The stator is provided with a main winding and an auxiliary winding which are in space quadrature. The excitation circuit is made up of the auxiliary winding, capacitance and diode rectifier bridge which supplies the conventional synchronous machine field winding. Although the generator is simple in structure, and has low voltage regulation, the generator needs frequent maintenance due to the presence of the collector ring and brushes.

Refs. [4, 5] presented single (three) phase self-excited synchronous generator. The stator is equipped with two separate windings having different pole numbers. One is the single (three) phase load winding and the other is the dc exciting winding. The rotor consists of the field coils short circuited with diodes. Although the structure is complicated, the output voltage can be kept constant over a wide range of load by adjusting the stator dc current.

This paper studies in detail the system proposed in ref. [2], fig. 1. Two rotor excitation modes are studied to indicate the effect of varying the diode configuration on the spectral analysis of output voltage waveform. Fig. 2 shows these proposed diode configuration.

Alexandria Engineering Journal. Vol. 41 (2002), No. 2, 233-244

2. Voltage equations in machine variables

The voltage equations in machine variables are based on the mathematical representation of the three-phase induction machine given in ref. [6, 7]. The winding arrangement for a 2-pole, three-phase, star-connected, symmetrical induction machine is shown in fig. 3. The stator windings are identical, sinusoidally distributed windings, displaced 120^0, with N_s equivalent turns and resistance r_s . The rotor windings will also be considered as three identical sinusoidally distributed windings, displaced 120^0, with N_r equivalent turns and resistance r_r. These voltages may be expressed as:

$$V_{as} = r_s i_{as} + p\lambda_{as}, \quad (1)$$

$$V_{bs} = r_s i_{bs} + p\lambda_{bs}, \quad (2)$$

$$V_{cs} = r_s i_{cs} + p\lambda_{cs}, \quad (3)$$

$$V_{ar} = r_r i_{ar} + p\lambda_{ar}, \quad (4)$$

$$V_{br} = r_r i_{br} + p\lambda_{br}, \text{ and} \quad (5)$$

$$V_{cr} = r_r i_{cr} + p\lambda_{cr}. \quad (6)$$

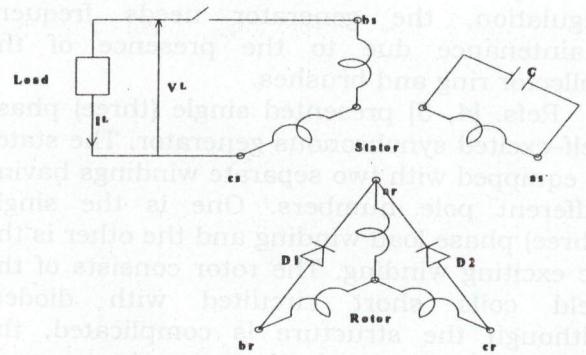

Fig. 1. Construction of BSESPSG using two diodes.

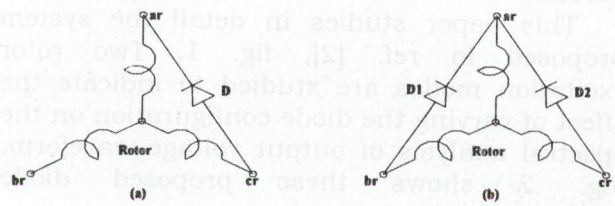

Fig. 2. Different rotor diode configuration (a) one-diode (b) two-diodes.

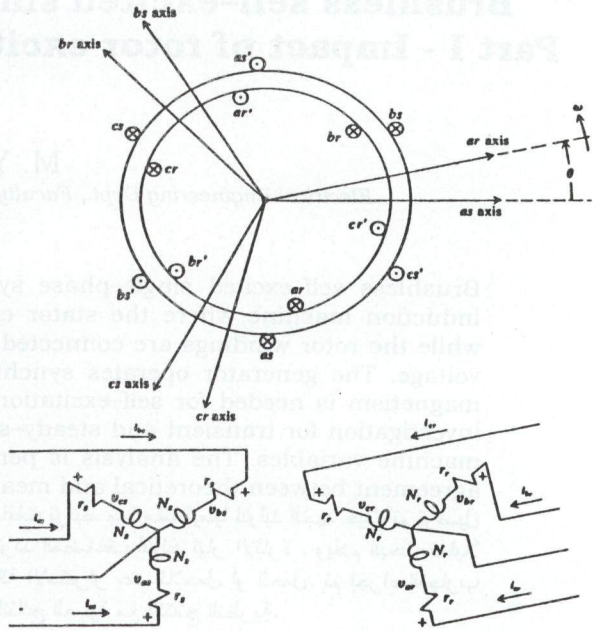

Fig. 3. Star-connected balanced 3-phase induction machine.

The flux linkages λ are related to machine inductances and currents by the following equations:

$$\lambda_{as} = L_s i_{as} - (1/2) L_{ms} (i_{bs} + i_{cs}) + L_{sr} [i_{ar} \cos\theta + i_{br} \cos\phi_1 + i_{cr} \cos\phi_2], \quad (7)$$

$$\lambda_{bs} = L_s i_{bs} - (1/2) L_{ms} (i_{as} + i_{cs}) + L_{sr} [i_{ar} \cos\phi_2 + i_{br} \cos\theta + i_{cr} \cos\phi_1], \quad (8)$$

$$\lambda_{cs} = L_s i_{cs} - (1/2) L_{ms} (i_{as} + i_{bs}) + L_{sr} [i_{ar} \cos\phi_1 + i_{br} \cos\phi_2 + i_{cr} \cos\theta], \quad (9)$$

$$\lambda_{ar} = L_r i_{ar} - (1/2) L_{mr} (i_{br} + i_{cr}) + L_{sr} [i_{as} \cos\theta + i_{bs} \cos\phi_2 + i_{cs} \cos\phi_1], \quad (10)$$

$$\lambda_{br} = L_r i_{br} - (1/2) L_{mr} (i_{ar} + i_{cr}) + L_{sr} [i_{as} \cos\phi_1 + i_{bs} \cos\theta + i_{cs} \cos\phi_2], \text{ and} \quad (11)$$

$$\lambda_{cr} = L_r i_{cr} - (1/2) L_{mr} (i_{ar} + i_{br}) + L_{sr} [i_{as} \cos\phi_2 + i_{bs} \cos\phi_1 + i_{cs} \cos\theta]. \quad (12)$$

Where;

$L_s = L_{Ls} + L_{ms}$,

$L_r = L_{Lr} + L_{mr}$,

$L_{ms} = (2/3) M$,

$L_{mr} = (N_r / N_s)^2 L_{ms}$, and

$L_{sr} = (N_r / N_s) L_{ms}$.

3. Saturation representation

For satisfactory modelling of this machine, saturation in the iron parts must be taken into account. Magnetising inductance M and related machine inductances can be determined by evaluating the magnitude of air gap mmf aided with d–q transformation. In such case the equivalent air gap mmf in the d–q axis as monitored by equivalent stator current assuming rotor rotating reference frame is given by [7]:

$$I_d = (2/3)[i_{as}\cos\theta + i_{bs}\cos\phi_2 + i_{cs}\cos\phi_1 + (N_r/N_s)(i_{ar}+i_{br}\cos(-2\pi/3)+i_{cr}\cos(2\pi/3))], \quad (13)$$

$$I_q = (2/3)[i_{as}\sin\theta+i_{bs}\sin\phi_2+i_{cs}\sin\phi_1 + (N_r/N_s)(i_{br}\sin(-2\pi/3) + i_{cr}\sin(2\pi/3))]. \quad (14)$$

Having determined the equivalent values of d–q axis currents, the peak value of magnetising current I_M is then given by:

$$I_M = \sqrt{I_d^2 + I_q^2}\ . \quad (15)$$

From open–circuit test, the relationship between the rms magnetising current I_m and magnetising reactance X_M is plotted. Then the relationship between $I_M = \sqrt{2}\, I_m$ and X_M is then plotted. Therefore calculating I_M using eq. (15) determines the corresponding value of the magnetising reactance X_M and consequently other machine parameters will be calculated. The proposed generator is analysed using the above equations under the two configurations mentioned earlier.

4. One–diode configuration

For this connection $i_{br} = 0$ & $i_{cr} = -i_{ar}$.

4.1. Excitation winding

$$V_c = -V_{as} = (1/C)\int i_{as}\,dt = Q/C, \quad (16)$$

where ,

$$Q = \int i_{as}\,dt \quad \text{i.e.} \quad pQ = i_{as}. \quad (17)$$

Substituting eq. (1) into eq. (16) we get:

$$L_s\, pi_{as} = -r_s\, i_{as} - Q/C - \sqrt{3}\, L_{sr}\, p[\, i_{ar}\cos\phi_4\,]. \quad (18)$$

4.2. No-load analysis

Output winding

At no–load $i_{bs} = i_{cs} = 0$,

$$V_{NL} = V_{bs} - V_{cs} = 3L_{sr}\cos\phi_3\, pi_{ar} - 3L_{sr}\,\omega\sin\phi_3\, i_{ar}. \quad (19)$$

Rotor windings

Two states are possible.

- Diode D–OFF

$i_{ar} = 0$ & $i_D = 0$.

Substituting the above conditions into eqs. (17, 18) we get:

$$\begin{bmatrix} p\,i_{as} \\ pQ \end{bmatrix} = \begin{bmatrix} L_s & 0 \\ 0 & 1 \end{bmatrix}^{-1} \begin{bmatrix} -r_s & -1/C \\ 1 & 0 \end{bmatrix} \begin{bmatrix} i_{as} \\ Q \end{bmatrix}, \quad (20)$$

$$V_D = V_{cr} - V_{ar} = \sqrt{3}\, L_{sr}\,[\,\cos\phi_5\, pi_{as} - \omega\sin\phi_5\, i_{as}\,]. \quad (21)$$

- Diode D–ON

$i_D = i_{ar}$,

$V_D = V_{cr} - V_{ar} = 0$.

Substituting the above conditions into eqs. (17, 18) , (4 and 6) we get :

$$\begin{bmatrix} pi_{as} \\ pi_{ar} \\ pQ \end{bmatrix} = \begin{bmatrix} L_s & \sqrt{3}L_{sr}\cos\phi_4 & 0 \\ \sqrt{3}L_{sr}\cos\phi_4 & 2L_{rr} & 0 \\ 0 & 0 & 1 \end{bmatrix}^{-1} \times \begin{bmatrix} -r_s & \sqrt{3}L_{sr}\omega\sin\phi_4 & -1/C \\ \sqrt{3}L_{sr}\omega\sin\phi_4 & -2r_r & 0 \\ 1 & 0 & 0 \end{bmatrix} \begin{bmatrix} i_{as} \\ i_{ar} \\ Q \end{bmatrix}. \quad (22)$$

where $L_{rr} = L_r + (1/2)\, L_{mr}$.

4.3. Load analysis

Output winding

With load $I_L = i_{cs} = -i_{bs}$,

$$V_L = V_{bs} - V_{cs}$$
$$= 2\, r_s\, i_{bs} + 2\, L_{ss}\, pi_{bs} + 3\, L_{sr} \cos\phi_3\, pi_{ar} - 3\, L_{sr}\, \omega \sin\phi_3\, i_{ar}, \quad (23)$$

$$= - R_L\, i_{bs} - L_L\, pi_{bs}, \quad (24)$$

where $L_{ss} = L_s + (1/2)\, L_{ms}$

Rotor windings

- Diode D–OFF

$i_{ar} = 0$ & $i_D = 0$.

Substituting the above conditions into eqs. (17, 18) and equating eqs. (23) and (24) we get:

$$\begin{bmatrix} pi_{as} \\ pi_{ar} \\ pQ \\ pi_{bs} \end{bmatrix} = \begin{bmatrix} L_s & \sqrt{3} L_{sr}\cos\phi_4 & 0 & 0 \\ \sqrt{3} L_{sr}\cos\phi_4 & 2L_{rr} & 0 & 3L_{sr}\cos\phi_3 \\ 0 & 0 & 1 & 0 \\ 0 & 3L_{sr}\cos\phi_3 & 0 & 2L_{ss}+L_L \end{bmatrix}^{-1} \times$$
$$\begin{bmatrix} -r_s & \sqrt{3} L_{sr}\,\omega \sin\phi_4 & -1/C & 0 \\ \sqrt{3} L_{sr}\,\omega \sin\phi_4 & -2r_r & 0 & 3L_{sr}\,\omega \sin\phi_3 \\ 1 & 0 & 0 & 0 \\ 0 & 3L_{sr}\,\omega \sin\phi_3 & 0 & -(2r_s + R_L) \end{bmatrix} \begin{bmatrix} i_{as} \\ i_{ar} \\ Q \\ i_{bs} \end{bmatrix} \quad (27)$$

5. Two-diode configuration

For this connection $i_{ar} = -(i_{br} + i_{cr})$

5.1. Excitation winding

$$V_c = - V_{as} = (1/C) \int i_{as}\, dt = Q/C, \quad (28)$$

where
$Q = \int i_{as}\, dt$ i.e. $pQ = i_{as}$. (29)

Substituting eq. (1) into eq. (28) we get:

$$L_s\, pi_{as} = - r_s\, i_{as} - Q/C - L_{sr}\, p[\, i_{ar} \cos\theta + i_{br} \cos\phi_1 + i_{cr} \cos\phi_2\,]. \quad (30)$$

$$\begin{bmatrix} pi_{as} \\ pQ \\ pi_{bs} \end{bmatrix} = \begin{bmatrix} L_s & 0 & 0 \\ 0 & 1 & 0 \\ 0 & 0 & 2L_{ss}+L_L \end{bmatrix}^{-1} \begin{bmatrix} -r_s & -1/C & 0 \\ 1 & 0 & 0 \\ 0 & 0 & -(2r_s+R_L) \end{bmatrix} \begin{bmatrix} i_{as} \\ Q \\ i_{bs} \end{bmatrix}, \quad (25)$$

$$V_D = V_{cr} - V_{ar}$$
$$= \sqrt{3}\, L_{sr} \cos\phi_5\, pi_{as} + 3\, L_{sr} \cos\phi_1\, pi_{bs} - \sqrt{3}\, L_{sr}\, \omega \sin\phi_5\, i_{as} - 3\, L_{sr}\, \omega \sin\phi_1\, i_{bs}. \quad (26)$$

- Diode D–ON

$i_D = i_{ar}$,

$V_D = V_{cr} - V_{ar} = 0$.

Substituting the above conditions into eqs. (17, 18), (4) and (6) and equating eqs. (23) and (24) we get:

5.2. No-load analysis

Output winding
At no-load $i_{bs} = i_{cs} = 0$,

$$V_{NL} = V_{bs} - V_{cs}$$
$$= \sqrt{3}\, L_{sr}[\cos\phi_6\, pi_{ar} + \cos\phi_4\, pi_{br} + \cos\phi_7\, pi_{cr}] - \sqrt{3}\, L_{sr}\omega[\sin\phi_6\, i_{ar} + \sin\phi_4\, i_{br} + \sin\phi_7\, i_{cr}]. \quad (31)$$

Rotor windings
Four states are possible.
- Diodes D1–OFF & D2– OFF

$i_{ar} = i_{br} = i_{cr} = 0$,
$i_{D1} = 0$ & $i_{D2} = 0$.

Substituting the above conditions into eqs. (29, 30) we get:

$$\begin{bmatrix} p\,i_{as} \\ pQ \end{bmatrix} = \begin{bmatrix} L_s & 0 \\ 0 & 1 \end{bmatrix}^{-1} \begin{bmatrix} -r_s & -1/C \\ 1 & 0 \end{bmatrix} \begin{bmatrix} i_{as} \\ Q \end{bmatrix}, \quad (32)$$

$$V_{D1} = V_{br} - V_{ar} = \sqrt{3}\ L_{sr}\ [\cos\phi_7\ p i_{as} - \omega \sin\phi_7\ i_{as}\ ], \quad (33)$$

$$V_{D2} = V_{cr} - V_{ar} = \sqrt{3}\ L_{sr}\ [\cos\phi_5\ p i_{as} - \omega \sin\phi_5\ i_{as}\ ]. \quad (34)$$

- Diode D1–ON & D2–OFF

$i_{D1} = -\,i_{br}$ & $i_{D2} = 0$,
$i_{ar} = -\,i_{br}$ & $i_{cr} = 0$,
$V_{D1} = V_{br} - V_{ar} = 0$.
Substituting the above conditions into eqs. (4,5,29, 30) we get:

$$\begin{bmatrix} p\,i_{as} \\ p\,i_{br} \\ pQ \end{bmatrix} = \begin{bmatrix} L_s & \sqrt{3}L_{sr}\cos\phi_7 & 0 \\ \sqrt{3}L_{sr}\cos\phi_7 & 2L_{rr} & 0 \\ 0 & 0 & 1 \end{bmatrix}^{-1} \times \begin{bmatrix} -r_s & \sqrt{3}L_{sr}\omega\sin\phi_7 & -1/C \\ \sqrt{3}L_{sr}\omega\sin\phi_7 & -2r_r & 0 \\ 1 & 0 & 0 \end{bmatrix} \begin{bmatrix} i_{as} \\ i_{br} \\ Q \end{bmatrix} \quad (35)$$

$$V_{D2} = V_{cr} - V_{ar} = r_r\, i_{br} + L_{rr}\, p i_{br} + \sqrt{3}\ L_{sr}\ [\cos\phi_5\ p i_{as} - \omega \sin\phi_5\ i_{as}\ ]. \quad (36)$$

$$\begin{bmatrix} pi_{as} \\ pi_{br} \\ pi_{cr} \\ pQ \end{bmatrix} = \begin{bmatrix} L_s & \sqrt{3}L_{sr}\cos\phi_7 & \sqrt{3}L_{sr}\cos\phi_5 & 0 \\ \sqrt{3}L_{sr}\cos\phi_7 & 2L_{rr} & L_{rr} & 0 \\ \sqrt{3}L_{sr}\cos\phi_5 & L_{rr} & 2L_{rr} & 0 \\ 0 & 0 & 0 & 1 \end{bmatrix}^{-1} \times \begin{bmatrix} -r_s & \sqrt{3}L_{sr}\omega\sin\phi_7 & \sqrt{3}L_{sr}\omega\sin\phi_5 & -1/C \\ \sqrt{3}L_{sr}\omega\sin\phi_7 & -2r_r & -r_r & 0 \\ \sqrt{3}L_{sr}\omega\sin\phi_5 & -r_r & -2r_r & 0 \\ 1 & 0 & 0 & 0 \end{bmatrix} \begin{bmatrix} i_{as} \\ i_{br} \\ i_{cr} \\ Q \end{bmatrix} \quad (39)$$

5.3. Load analysis

Output winding
With load $I_L = i_{cs} = -\,i_{bs}$

- Diode D1–OFF & D2– ON

$i_{D1} = 0$ & $i_{D2} = -i_{cr}$,
$i_{ar} = -i_{cr}$ & $i_{br} = 0$,
$V_{D2} = V_{cr} - V_{ar} = 0$.

Substituting the above conditions into eqs. (4,6,29,30) we get :

$$\begin{bmatrix} p_{ias} \\ p_{icr} \\ pQ \end{bmatrix} = \begin{bmatrix} L_s & \sqrt{3}L_{sr}\cos\phi_5 & 0 \\ \sqrt{3}L_{sr}\cos\phi_5 & 2L_{rr} & 0 \\ 0 & 0 & 1 \end{bmatrix}^{-1} \times \begin{bmatrix} -r_s & \sqrt{3}L_{sr}\omega\sin\phi_5 & -1/C \\ \sqrt{3}L_{sr}\omega\sin\phi_5 & -2r_r & 0 \\ 1 & 0 & 0 \end{bmatrix} \begin{bmatrix} ias \\ icr \\ Q \end{bmatrix} \quad (37)$$

$$V_{D1} = V_{br} - V_{ar} = r_r\, i_{cr} + L_{rr}\, p i_{cr} + \sqrt{3}\ L_{sr}\ [\cos\phi_7\ p i_{as} - \omega \sin\phi_7\ i_{as}\ ]. \quad (38)$$

- Diode D1–ON & D2–ON

$i_{D1} = -\,i_{br}$ & $i_{D2} = -\,i_{cr}$,
$i_{ar} = -\,(\,i_{br} + i_{cr}\,)$,
$V_{D1} = V_{br} - V_{ar} = 0$,
$V_{D2} = V_{cr} - V_{ar} = 0$.

Substituting the above conditions into eqs. (4,5,6,29,30) we get:

$$V_L = V_{bs} - v_{cs} = 2\, r_s\, i_{bs} + 2\, L_{ss}\, p i_{bs} + \sqrt{3}\ L_{sr}[\cos\phi_6\ p i_{ar} + \cos\phi_4\ p i_{br} + \cos\phi_7\ p i_{cr}] - \sqrt{3}\ L_{sr}\omega[\sin\phi_6\ i_{ar} + \sin\phi_4\ i_{br} + \sin\phi_7\ i_{cr}], \quad (40)$$

$$= - R_L\, i_{bs} - L_L\, pi_{bs}. \qquad (41)$$

Rotor windings

-Diodes D1–OFF & D2– OFF

$i_{ar} = i_{br} = i_{cr} = 0,$
$i_{D1} = 0$ & $i_{D2} = 0.$

Substituting the above conditions into eqs. (29,30) and equating eqs. (39) and (40) we get:

$$\begin{bmatrix} p_{ias} \\ pQ \\ p_{ibs} \end{bmatrix} = \begin{bmatrix} L_s & 0 & 0 \\ 0 & 1 & 0 \\ 0 & 0 & 2L_{ss}+L_L \end{bmatrix}^{-1} \begin{bmatrix} -r_s & -1/C & 0 \\ 1 & 0 & 0 \\ 0 & 0 & -(2r_s+R_L) \end{bmatrix} \begin{bmatrix} i_{as} \\ Q \\ i_{bs} \end{bmatrix}, \qquad (42)$$

$$\begin{bmatrix} pi_{as} \\ pi_{br} \\ pQ \\ pi_{bs} \end{bmatrix} = \begin{bmatrix} L_s & \sqrt{3}L_{sr}\cos\phi_7 & 0 & 0 \\ \sqrt{3}L_{sr}\cos\phi_7 & 2L_{rr} & 0 & 3L_{sr}\cos\phi_8 \\ 0 & 0 & 1 & 0 \\ 0 & 3L_{sr}\cos\phi_8 & 0 & 2L_{ss}+L_L \end{bmatrix}^{-1} \times$$

$$\begin{bmatrix} -r_s & \sqrt{3}L_{sr}\omega\sin\phi_7 & -1/C & 0 \\ \sqrt{3}L_{sr}\omega\sin\phi_7 & -2r_r & 0 & 3L_{sr}\omega\sin\phi_8 \\ 1 & 0 & 0 & 0 \\ 0 & 3L_{sr}\omega\sin\phi_8 & 0 & -(2r_s+R_L) \end{bmatrix} \begin{bmatrix} i_{as} \\ i_{br} \\ Q \\ i_{bs} \end{bmatrix}, \qquad (45)$$

$$V_{D2} = V_{cr} - V_{ar}$$
$$= r_r\, i_{br} + L_{rr}\, pi_{br} + \sqrt{3}\, L_{sr}\,[\cos\phi_5\, pi_{as} - \omega \sin\phi_5\, i_{as}] + 3\, L_{sr}\,[\cos\phi_1\, pi_{bs} - \omega \sin\phi_1\, i_{bs}]. \qquad (46)$$

$$\begin{bmatrix} pi_{as} \\ pi_{cr} \\ pQ \\ pi_{bs} \end{bmatrix} = \begin{bmatrix} L_s & \sqrt{3}L_{sr}\cos\phi_5 & 0 & 0 \\ \sqrt{3}L_{sr}\cos\phi_5 & 2L_{rr} & 0 & 3L_{sr}\cos\phi_1 \\ 0 & 0 & 1 & 0 \\ 0 & 3L_{sr}\cos\phi_1 & 0 & 2L_{ss}+L_L \end{bmatrix}^{-1} \times$$

$$\begin{bmatrix} -r_s & \sqrt{3}L_{sr}\omega\sin\phi_5 & -1/C & 0 \\ \sqrt{3}L_{sr}\omega\sin\phi_5 & -2r_r & 0 & 3L_{sr}\omega\sin\phi_1 \\ 1 & 0 & 0 & 0 \\ 0 & 3L_{sr}\omega\sin\phi_1 & 0 & -(2r_s+R_L) \end{bmatrix} \begin{bmatrix} i_{as} \\ i_{cr} \\ Q \\ i_{bs} \end{bmatrix}, \qquad (47)$$

$$V_{D1} = V_{br} - V_{ar}$$
$$= \sqrt{3}\, L_{sr}\,[\cos\phi_7\, pi_{as} - \omega \sin\phi_7\, i_{as}] + 3\, L_{sr}\,[\cos\phi_8\, pi_{bs} - \omega \sin\phi_8\, i_{bs}], \qquad (43)$$

$$V_{D2} = V_{cr} - V_{ar}$$
$$= \sqrt{3}\, L_{sr}\,[\cos\phi_5\, pi_{as} - \omega \sin\phi_5\, i_{as}] + 3\, L_{sr}\,[\cos\phi_1\, pi_{bs} - \omega \sin\phi_1\, i_{bs}]. \qquad (44)$$

-Diode D1–ON & D2–OFF

$i_{D1} = - i_{br}$ & $i_{D2} = 0,$
$i_{ar} = - i_{br}$ & $i_{cr} = 0,$
$V_{D1} = V_{br} - V_{ar} = 0.$

Substituting the above conditions into eqs. (4,5,29,30), and equating eqs. ((39) and (40)we get:

-Diode D1–OFF & D2– ON

$i_{D1} = 0$ & $i_{D2} = - i_{cr},$
$i_{ar} = - i_{cr}$ & $i_{br} = 0,$
$V_{D2} = V_{cr} - V_{ar} = 0.$

Substituting the above conditions into eqs. (4,5,29,30) and equating eqs. (39,40) we get:

$$V_{D1} = V_{br} - V_{ar} = r_r i_{cr} + L_{rr} pi_{cr} + \sqrt{3}\, L_{sr} [\cos\phi_7\, pi_{as} - \omega \sin\phi_7\, i_{as}] + 3 L_{sr} [\cos\phi_8\, pi_{bs} - \omega \sin\phi_8\, i_{bs}]. \quad (48)$$

-Diode D1–ON & D2–ON

$i_{D1} = -i_{br}$ & $i_{D2} = -i_{cr}$,
$i_{ar} = -(i_{br} + i_{cr})$,
$V_{D1} = V_{br} - V_{ar} = 0$,
$V_{D2} = V_{cr} - V_{ar} = 0$.

Substituting the above conditions into eqs. (4,5,6,29,30) and equating eqs. (39) and (40) we get:

$$\begin{bmatrix} pi_{as} \\ pi_{br} \\ pi_{cr} \\ pQ \\ pi_{bs} \end{bmatrix} = \begin{bmatrix} L_s & \sqrt{3}L_{sr}\cos\phi_7 & \sqrt{3}L_{sr}\cos\phi_5 & 0 & 0 \\ \sqrt{3}L_{sr}\cos\phi_7 & 2L_{rr} & L_{rr} & 0 & 3L_{sr}\cos\phi_8 \\ \sqrt{3}L_{sr}\cos\phi_5 & L_{rr} & 2L_{rr} & 0 & 3L_{sr}\cos\phi_1 \\ 0 & 0 & 0 & 1 & 0 \\ 0 & 3L_{sr}\cos\phi_8 & 3L_{sr}\cos\phi_1 & 0 & 2L_{ss}+L_L \end{bmatrix}^{-1} \times \begin{bmatrix} -r_s & \sqrt{3}L_{sr}\omega\sin\phi_7 & \sqrt{3}L_{sr}\omega\sin\phi_5 & -1/C & 0 \\ \sqrt{3}L_{sr}\omega\sin\phi_7 & -2r_r & -r_r & 0 & 3L_{sr}\omega\sin\phi_8 \\ \sqrt{3}L_{sr}\omega\sin\phi_5 & -r_r & -2r_r & 0 & 3L_{sr}\omega\sin\phi_1 \\ 1 & 0 & 0 & 0 & 0 \\ 0 & 3L_{sr}\omega\sin\phi_8 & 3L_{sr}\omega\sin\phi_1 & 0 & -(2r_s + R_L) \end{bmatrix} \begin{bmatrix} i_{as} \\ i_{br} \\ i_{cr} \\ Q \\ i_{bs} \end{bmatrix} \quad (49)$$

6. Experimental and simulation results

The experimental set up is made of a slip ring, three–phase induction machine whose specifications are: 4 –pole, 220/380 V Δ/Y, 11.3/6.5 A, 2.2 kW, 50 Hz, 1390 rpm, rotor: 100 V Y, 14 A. The phase parameters as obtained by standard tests (no load and blocked rotor tests) are as follows:

$r_s = 1.92\ \Omega$, $r_r = 0.32\ \Omega$, $L_{Ls} = 9.3265$ mH,
$L_{Lr} = 0.78304$ mH, $(N_r / N_s) = 100 / 345$
$M = 286.48$ mH $\quad I_M \le 1.77$ A
$M = 359.9 - 41.48\, I_M$ mH $\quad 1.77 < I_M \le 4.7$A
$M = 245.8 - 17.2\, I_M$ mH $\quad 4.7 < I_M \le 7.8$ A
$M = 111.6$ mH $\quad I_M > 7.8$ A

The induction machine is connected in the BSESPSG mode as shown in fig. 1 and mechanically coupled to a compounded dc motor to adjust the speed of rotation. To obtain an output voltage having a frequency f=50 Hz, the speed of rotation is adjusted to 1500 rpm. Voltage building up in this generator is a transient phenomenon and it takes place by virtue of residual magnetism present in the magnetic material. The residual magnetism should be represented by assuming initial value for excitation current i_{as} equal to an arbitrary value say i_{as} = 50 mA. Self–excitation of BSESPSG is achieved by using an excitation winding where a capacitor is used to provide the leading reactive power required. Computer programs written in Pascal were developed for simulation purposes. These programs are used for predicting the performance of the BSESPSG. For the simulation results, Euler method of numerical integration was used. The time increment for numerical integration Δt was chosen to be (1 / 500 f), i.e $\Delta t = 4 \times 10^{-5}$ sec.

For comparison purposes, results obtained from real system are compared with those obtained from digital simulation. Performance characteristics of BSESPSG were determined under no–load and loading conditions.

Fig. 4 shows the experimental and simulation results for one–diode configuration at no–load with an excitation capacitor C = 40μF. fig. 5 shows the case of two–diode configuration, with an excitation capacitor C = 80μF. From fig. 4, it is observed that the output no–load voltage is highly distorted.

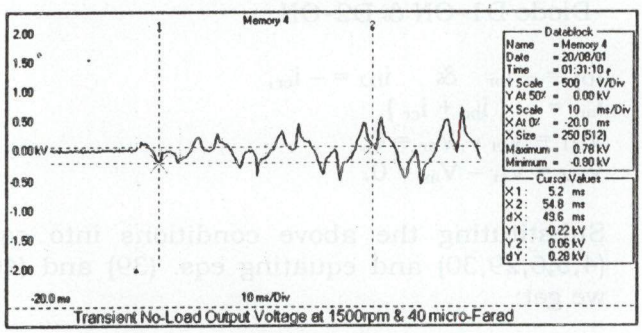

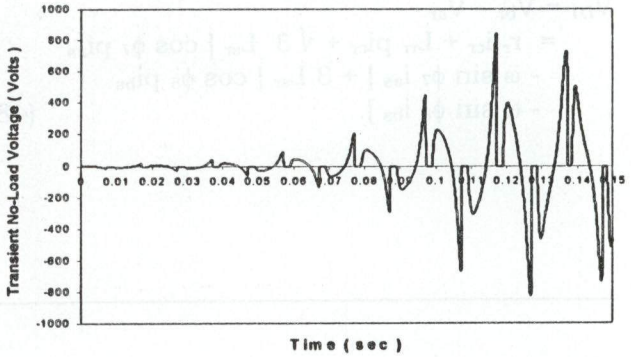

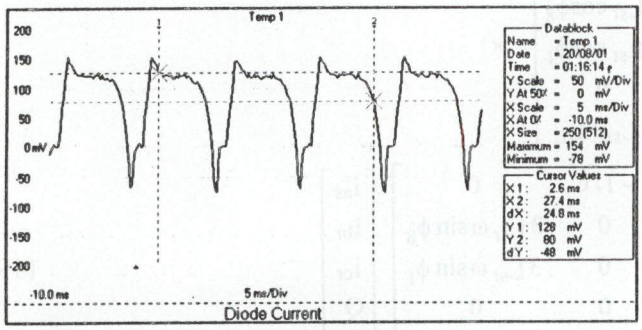

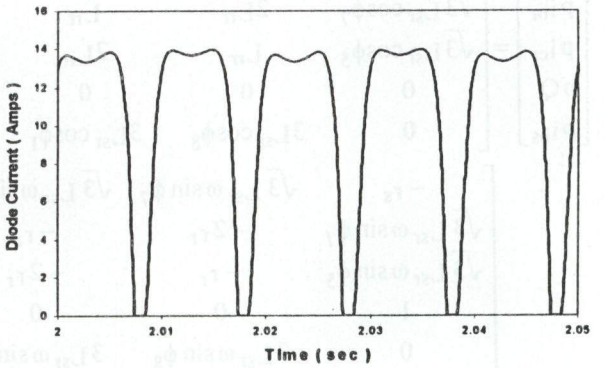

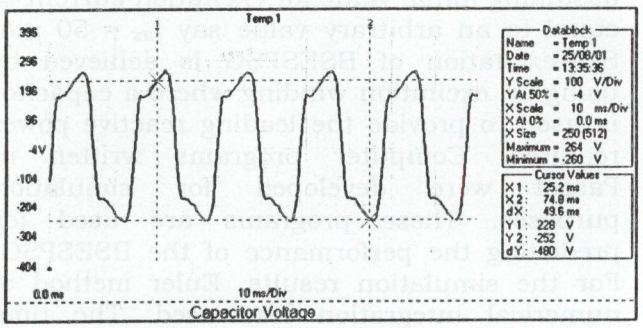

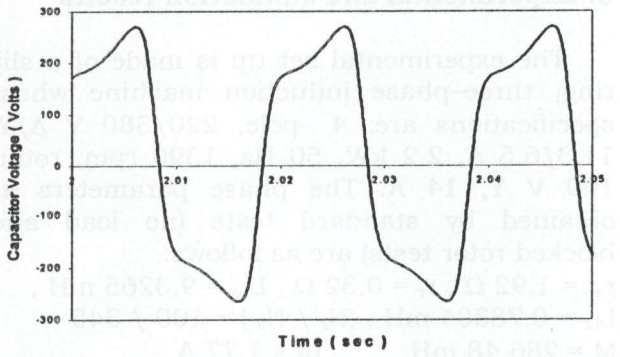

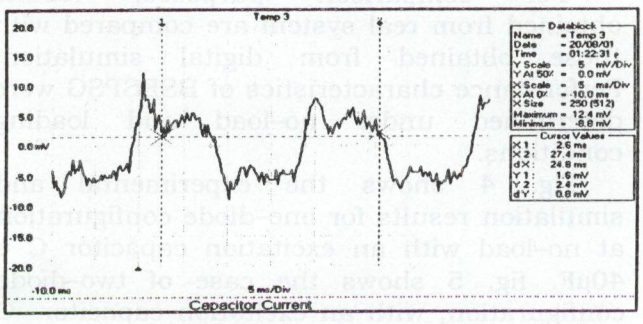

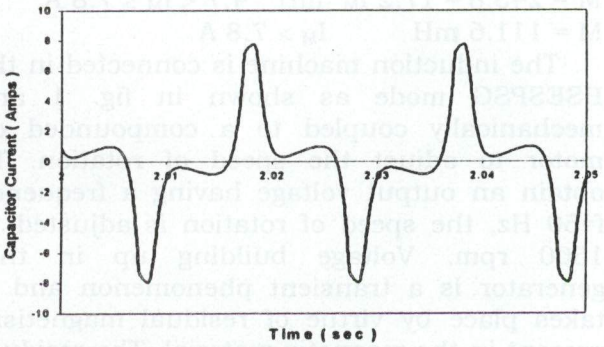

Fig. 4. Experimental and simulation results of one-diode configuration at no-load.

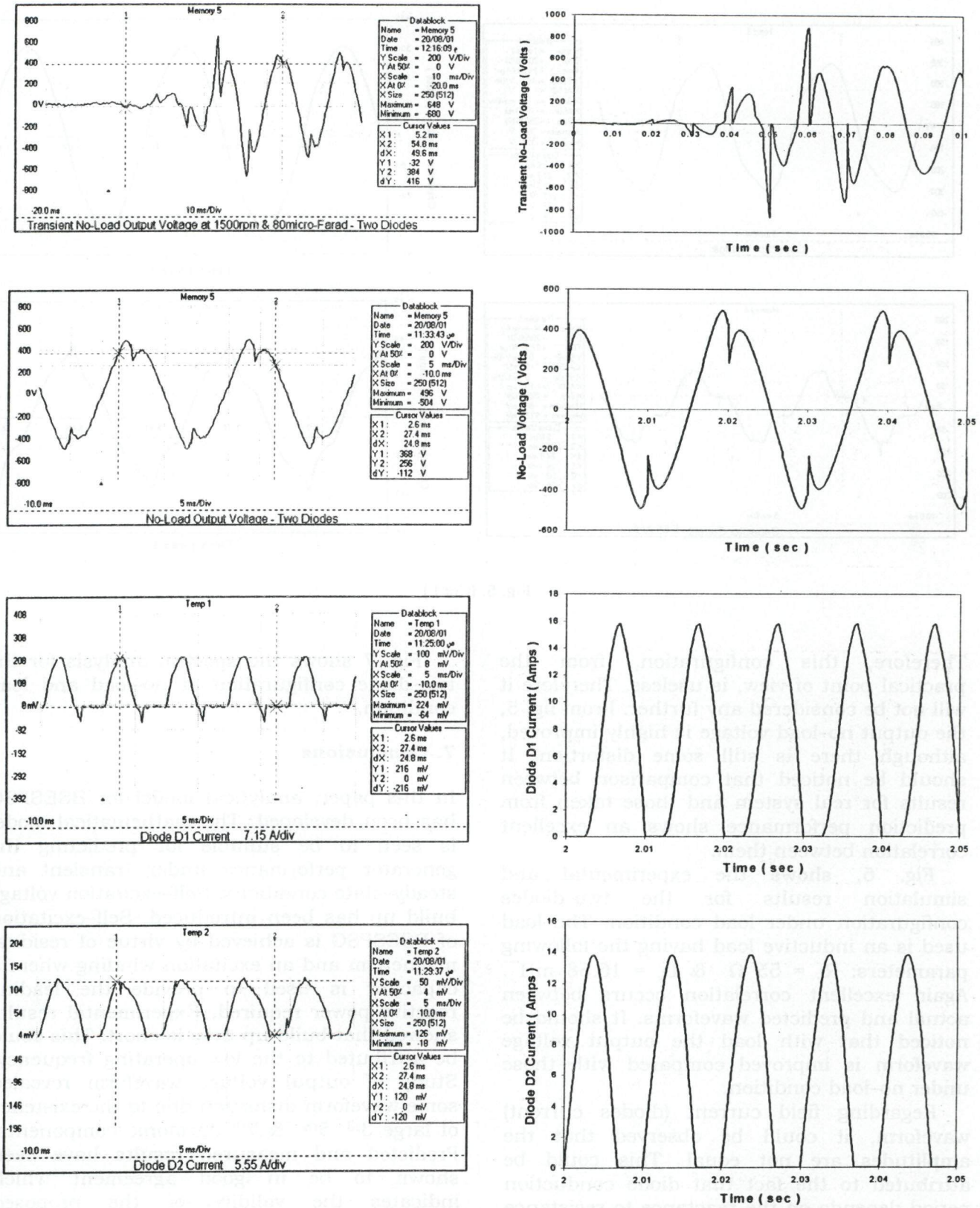

Fig. 5. Experimental and simulation results for two-diode configuration at no-load.

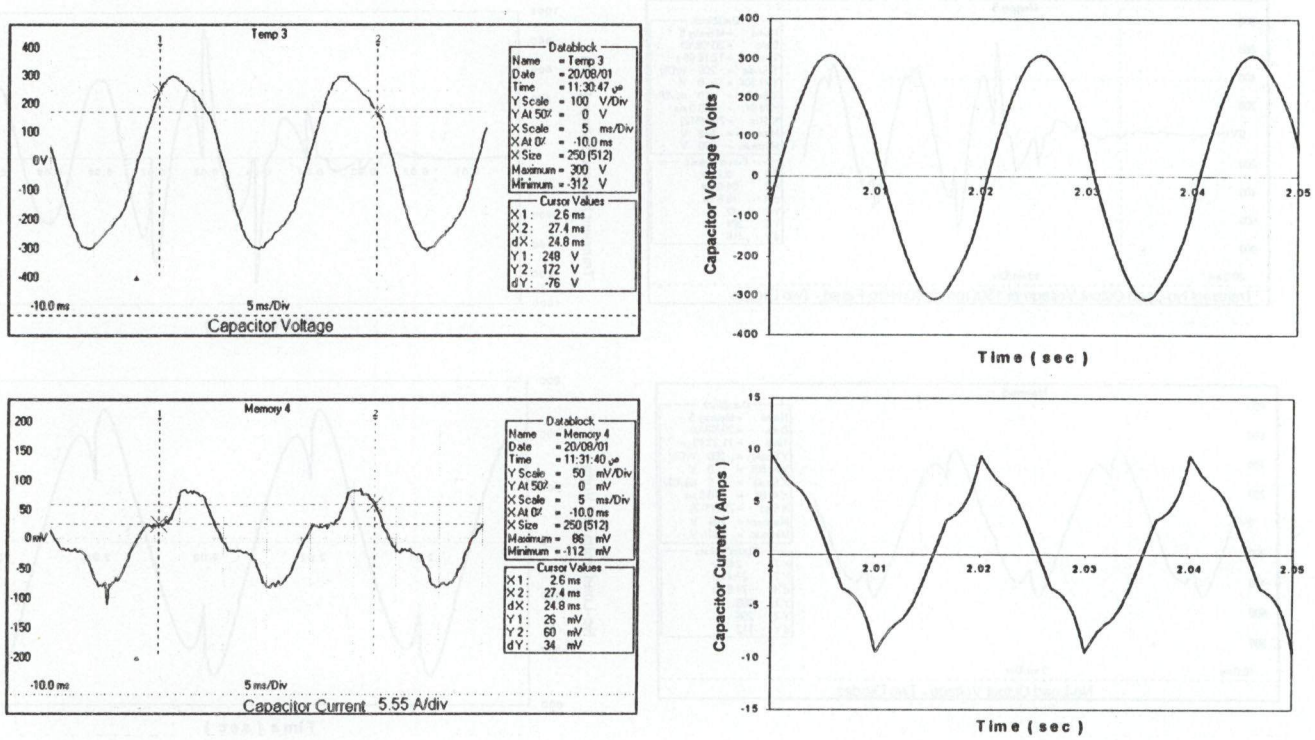

Fig. 5. (Cont.)

Therefore, this configuration, from the practical point of view, is useless. Therefore it will not be considered any further. From fig. 5, the output no–load voltage is highly improved, although there is still some distortion. It should be noticed that comparison between results for real system and those taken from prediction performance shows an excellent correlation between them.

Fig. 6, shows the experimental and simulation results for the two–diodes configuration under load condition. The load used is an inductive load having the following parameters: R_L = 55 Ω & L_L = 16.58 mH . Again excellent correlation occurs between actual and predicted waveforms. It should be noticed that with load the output voltage waveform is improved compared with those under no–load condition.

Regarding field current (diodes current) waveform, it could be observed that the amplitudes are not equal. This could be attributed to the fact that diode conduction period depends on the reactance to resistance ratio of field circuit.

Fig. 7 shows the spectral analysis for the two–diode configuration at no–load and load condition.

7. Conclusions

In this paper, analytical model for BSESPSG has been developed. The mathematical model is seen to be suitable for predicting the generator performance under transient and steady–state conditions. Self–excitation voltage build up has been introduced. Self–excitation of BSESPSG is achieved by virtue of residual magnetism and an excitation winding where a capacitor is used to provide the leading reactive power required. Experimental results showed that build up time is short. This could be attributed to the low operating frequency. Study of output voltage waveform revealed some waveform distortion due to the existence of large 3rd, 5th & 7th harmonic components. Predicted and measured results have been shown to be in good agreement which indicates the validity of the proposed analytical model.

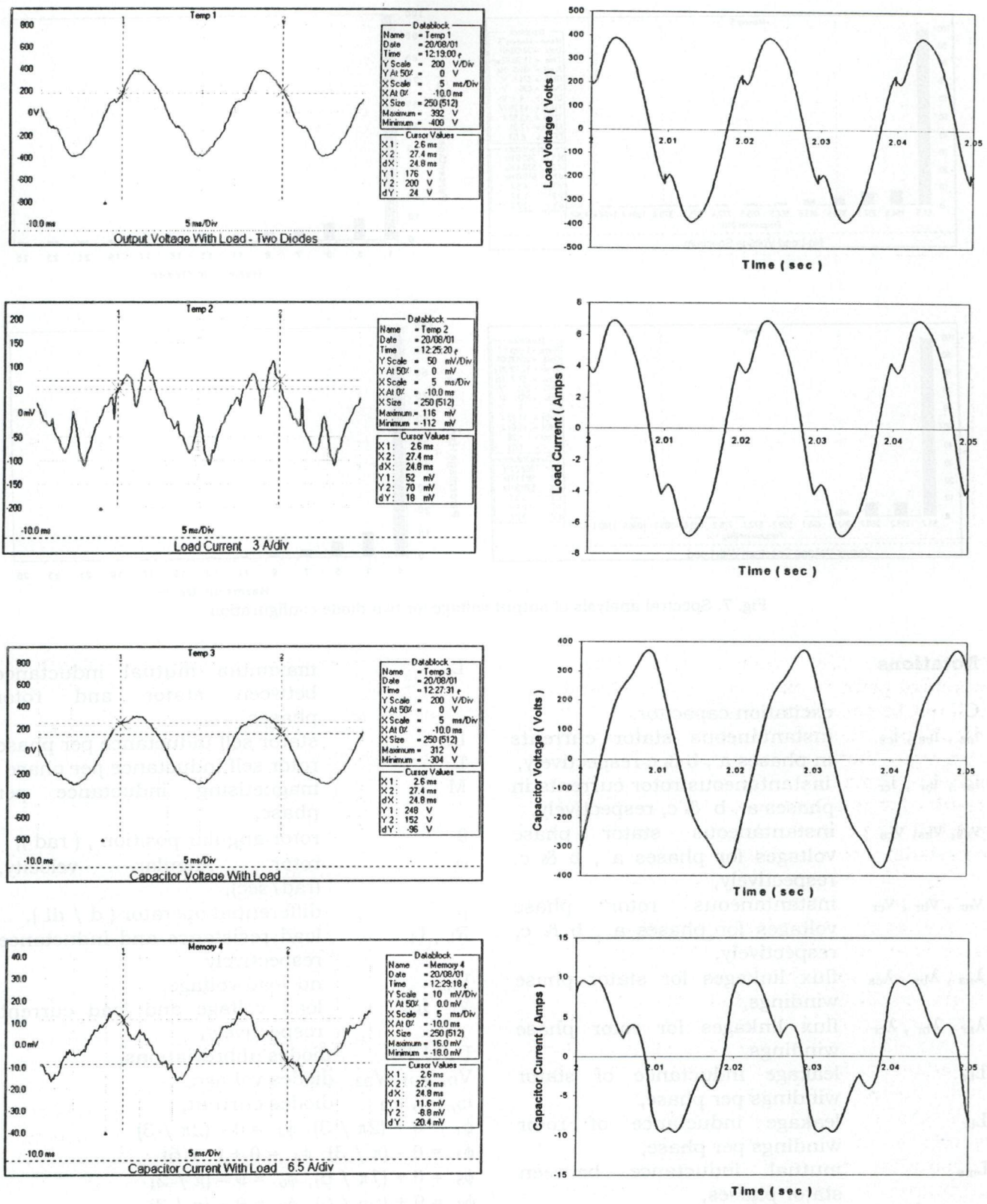

Fig. 6. Experimental and simulation results of two-diode configuration with load.

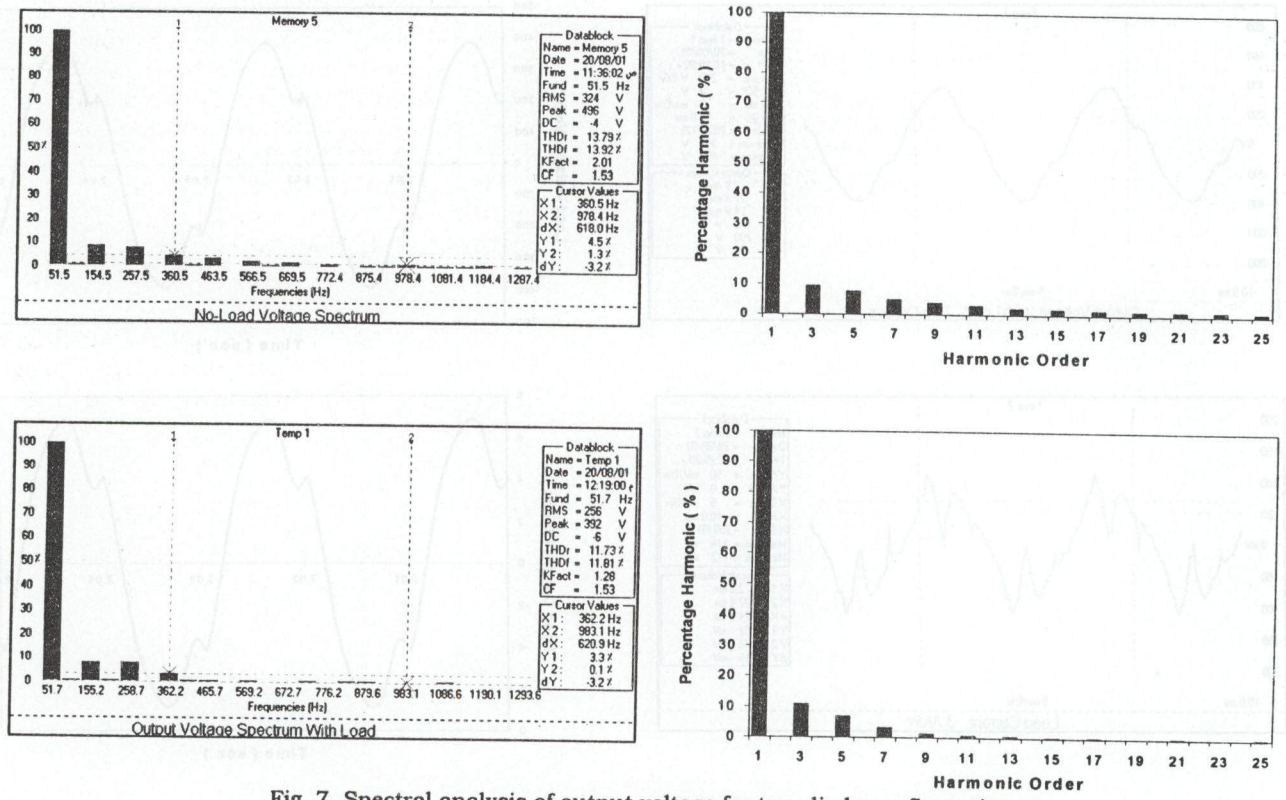

Fig. 7. Spectral analysis of output voltage for two-diode configuration.

Notations

C	excitation capacitor,
i_{as} , i_{bs} , i_{cs}	instantaneous stator currents in phases a , b & c respectively,
i_{ar} , i_{br} , i_{cr}	instantaneous rotor currents in phases a , b & c, respectively,
v_{as}, v_{bs}, v_{cs}	instantaneous stator phase voltages for phases a , b & c, respectively,
v_{ar} , v_{br} , v_{cr}	instantaneous rotor phase voltages for phases a , b & c, respectively,
λ_{as} , λ_{bs} , λ_{cs}	flux linkages for stator phase windings,
λ_{ar} , λ_{br} , λ_{cr}	flux linkages for rotor phase windings,
L_{Ls}	leakage inductance of stator windings per phase,
L_{Lr}	leakage inductance of rotor windings per phase,
L_{ms}	mutual inductance between stator phases,
L_{mr}	mutual inductance between rotor phases,
L_{sr}	maximum mutual inductance between stator and rotor phases,
L_s	stator self inductance per phase
L_r	rotor self inductance per phase
M	magnetising inductance per phase,
θ	rotor angular position , (rad),
ω	rotor angular velocity, (rad/sec),
p	differential operator (d / dt),
R_L , L_L	load resistance and inductance respectively,
V_{NL}	no–load voltage,
V_L , I_L	load voltage and load current respectively,
D,D1,D2	diodes abbreviations,
V_D, V_{D1}, V_{D2}	diodes voltage,
i_D, i_{D1}, i_{D2}	diodes current,

$\phi_1 = \theta + (2\pi / 3)$, $\phi_2 = \theta - (2\pi / 3)$
$\phi_3 = \theta - (\pi / 3)$, $\phi_4 = \theta + (\pi / 6)$
$\phi_5 = \theta + (7\pi / 6)$, $\phi_6 = \theta - (\pi / 2)$
$\phi_7 = \theta + (5\pi / 6)$, $\phi_8 = \theta + (\pi / 3)$

References

[1] S. Nonaka and I. Muta, "Characteristics Of Brushless Self Excited Synchronous Generators," Electrical Engineering in Japan Vol. 91(4), pp. 41–51 (1971).

[2] E. S. Hamdi, "Brushless Self Excited Synchronous Machines," M.Sc. Thesis, Faculty of Engineering, Alexandria University, Egypt (1978).

[3] T. F. Chan, "A Self-Excited Single-Phase Synchronous Generator," Int. J. Elec. Eng. Educ., Vol. 23, pp. 273–281 (1986).

[4] S. Nonaka and K. Kesamaru, "Analysis of Voltage Adjustable Brushless Synchronous Generator Without Exciter," IEEE Trans. on Industry Applications, Vol. 25 (1), pp. 126–132 (1989).

[5] S. Nonaka, K. Kesamaru and K. Horita, "Analysis of Brushless Four-Pole Three-Phase Synchronous Generator Without Exciter by the Finite Element Method," IEEE Trans. on Industry Applications, Vol. 30 (3), pp. 615–620 (1994).

[6] P. C. Krause and C. H. Thomas, "Simulation of Symmetrical Induction Machinery," IEEE Trans. on Power Appt. and Systems, Vol. PAS-84 (11), pp. 1038–1053 (1965).

[7] Paul C. Krause, Oleg Wasynczuk and Scott D. Sudhoff, " Analysis Of Electric Machinery," IEEE Press, Chapters 1 & 4. (1995).

Received October 27, 2001
Accepted January 8, 2002